Hysteretic electroluminescence in organic light-emitting diodes for spin injection

G. Salis, S. F. Alvarado, M. Tschudy, T. Brunschwiler, and R. Allenspach
IBM Research, Zurich Research Laboratory, Säumerstrasse 4, 8803 Rüschlikon, Switzerland
(Received 31 March 2004; revised manuscript received 11 May 2004; published 12 August 2004)

Organic light-emitting diodes with ferromagnetic contacts are fabricated, and their emission intensity is studied at room temperature for parallel and antiparallel magnetization configuration of anode and cathode. Sweeping the magnetic field applied parallel to the electrode allows the magnetization of the two electrodes to be switched independently. The electroluminescence intensity for the antiparallel magnetic configuration is found to be enhanced as compared to the parallel one. We show that this increase is not evidence of spin injection but is a consequence of the magnetic-field dependence of the electroluminescence intensity combined with magnetic stray fields from the electrodes.

DOI: 10.1103/PhysRevB.70.085203 PACS number(s): 85.75.−d, 72.25.Hg, 78.60.Fi, 78.66.Qn

Spin lifetimes in organic materials are expected to be on the order of microseconds,[1] making these materials potentially useful for spin-based information-processing devices. An essential requirement for "spintronics" devices is the efficient injection of spin-polarized carriers from a ferromagnetic contact into the active material. In the case of semiconductors, such spin injection has been demonstrated by measuring the polarization of light generated by recombining carriers in a quantum well.[2] In III-V semiconductors, the degree of circular polarization of the emitted photons is coupled to the spin polarization of the recombining carriers due to optical selection rules for transitions between the spin-orbit split valence and the conduction-band.[3] This scheme is not applicable to organic light-emitting diodes (OLEDs), where the optical selection rules for electric dipole transitions are not determined by spin-orbit interaction and therefore the polarization of emitted photons is not directly related to the spin of the electron. However, simultaneous polarization of both electron and hole spins of recombining carriers may influence the OLED electroluminescence (EL) *intensity* because of the nonradiative nature of triplet excitons:[4] In the case of antiparallel configuration of electron and hole spins, the formation of singlet states is enhanced, increasing the luminescence intensity, whereas triplet states should dominate in parallel configuration, thus suppressing light emission. Spin-injection into OLEDs is the topic of increasing research activities.[4–7]

An important role is attributed to the interface between the ferromagnetic metal (FM) and the organic material. As has been shown for FM/semiconductor layers with Ohmic contacts, large differences in the conductivities of the layers prevent efficient spin injection.[8] For inorganic semiconductors it has been shown theoretically and experimentally that a tunnel barrier[9] or hot-carrier injection[10] circumvent the conductivity-mismatch problem and potentially allow large spin-injection efficiencies. This should also hold for our FM/organic interfaces (see experimental details below).

In this paper we investigate the EL intensity I of OLEDs with magnetic electrodes and find a dependence on the relative magnetization orientation of anode and cathode. We observe an enhancement of I for antiparallel magnetic configuration compared with the value for a parallel configuration. This could be an indication that the electron and hole spin-polarizations of the excitons are correlated with the magnetization of the corresponding electrodes. We compare the data with those of samples containing only one magnetic electrode, where no spin-dependent modulation of I is expected. In combination with an analysis of the magnitude of the effect as a function of the voltage applied across the OLED, we find evidence that in the samples discussed in this work the EL modulation originates from the magnetic stray fields emanating from the electrodes. We deduce an upper limit of 5×10^{-5} for the product of the spin polarization of electrons and holes attributable to spin injection.

We present results obtained with OLEDs that consist of an organic stack of tris(8-hydroxyquinolinato)aluminum (Alq_3) and 2,2′,7,7′-tetrakis(diphenylamino)-9,9′-spirobifluorene (STAD). Alq_3 serves as an electron-transporting and emitting material, whereas STAD is the hole-transporting material [Fig. 1(a)]. For the magnetic electrodes, we choose Ni and $Ni_{0.81}Fe_{0.19}$ (Py) because of the high degree of spin polarization at the Fermi level in these metals.[11,12] In addition, their coercive fields are very different, allowing us to establish parallel and antiparallel magnetization orientations of the electrodes. Several samples with the following anode/cathode combinations were fabricated: Al/Py, Ni/Py, and Ni/Ca. The OLEDs are made on glass substrates with prepatterned anodes prepared in a separate metal-deposition chamber. The thickness of the anode metal thin films is in the range of 50–70 nm. A thin Al_2O_3 layer is obtained by oxidizing a 1-nm-thick film of Al deposited on top of the anode. The final step in the preparation of the anode is the deposition of a thin film of fluorocarbon (CF_x) in a reactive sputter apparatus. The freshly prepared anode substrates are inserted into an Ar-filled glovebox. Next, the substrates are introduced into an appended evaporation chamber for organic-material and cathode deposition. The organic layers, deposited by thermal sublimation, consist of a 55-nm-thick film of STAD followed by 50 nm of Alq_3. A semitransparent cathode is made by depositing a thin film of LiF (approx. 0.5 nm thick) and a metal thin film of nominal thickness in the range of 6–9 nm and capped with a 2-nm-thick Al layer. The base pressure of the evaporation system is in the mid-10^{-7} mbar range. At the initial stages of the metal evaporation, the pressure increases up to

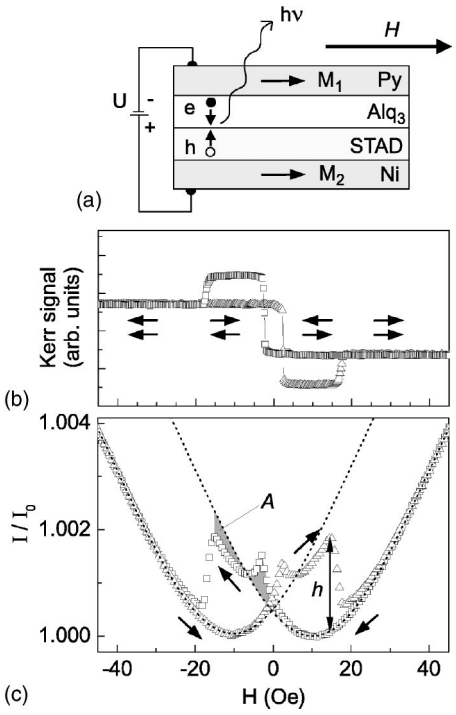

FIG. 1. (a) Schematic view of the thin-film OLED structure used in these studies. The magnetic field H is applied in the sample plane. (b) Magnetic hysteresis loop of the OLED with a Ni anode and Py cathode, as measured with the longitudinal magneto-optical Kerr effect. The two magnetic layers display different switching fields, enabling the parallel and antiparallel configuration of the magnetization (arrows). (c) Corresponding OLED intensity I vs H for up (triangles) and down (squares) sweeps shows intensity enhancement for the antiparallel magnetic configuration ($U=5.0$ V). Dotted lines are Lorentz fits to up and down sweeps in the magnetically saturated regions, defining two curves that are simply displaced in the direction of the field. The height h defines the relative intensity change at magnetization reversal of the Ni layer. Area A (shaded) is the difference between I/I_0 and the Lorentz fit, integrated over the region with antiparallel magnetization.

10^{-6} mbar. Anode and cathode overlap on an area of 2×3 mm^2, which is the size of the light-emissive region. Regarding the properties of the cathode, we have already shown that the intercalation of a LiF thin film between the organic and the metal electrode leads to a reduction of the barrier height at the interface from 1.1 to 0.4 eV.[13] In the present devices we have added a thin aluminium oxide buffer layer between the cathode and the LiF layer. Therefore we conclude that in these devices the cathodes are not Ohmic. Regarding the anodes, we performed a comparative study between devices having either FM or indium-thin oxide (ITO) anodes[14] and found that significantly lower operating voltages can be achieved when using ITO. This indicates a nonzero potential drop at the FM-organic interface, i.e., the anodes used in the devices here reported are not Ohmic. Therefore, we do not expect the conductivity mismatch[8] between FM electrodes and organic layers to prevent efficient spin injection in our devices. Further details on anode and cathode preparation will be published elsewhere. The OLEDs are encapsulated in Ar gas and extracted from the glovebox to perform the magnetic-field-dependent EL measurements. The modified anode and cathode configurations used in the OLEDs allow us to achieve voltage thresholds of 2–2.2 V for the onset of EL and current densities higher than 10^{-2} A/cm^2 for bias voltages below 6 V. This represents a considerable improvement when compared to typical OLEDs having transition-metal electrodes, where typical operating voltages are much higher.[4–6] The realization of low EL threshold and high current densities at low bias voltages is necessary for efficient spin injection into and detection in organic materials.

The EL intensity I of the OLEDs is measured at a constant bias U at room temperature using an unbiased Si photodiode as a detector. A magnetic field H is applied in the plane of the sample [Fig. 1(a)] monitored by an *in situ* Hall probe. The presented data of $I(H)$ is obtained by averaging over several hysteresis loops, whereby a slow drift of I with time has been corrected by using a linear approximation.

Figure 1(b) shows the magnetic hysteresis loop obtained by a longitudinal magnetooptical Kerr-effect measurement of a Ni/Py sample. It reveals two distinct transitions per sweep direction, corresponding to the magnetization reversal of the Py and Ni layers occurring at $\sim$2.5 and 17 Oe, respectively. By appropriate sweeps of H it is therefore possible to switch the magnetization of electrode and cathode independently into parallel and antiparallel configuration, as indicated by the arrows in Fig. 1(b).

In Fig. 1(c), data of I/I_0 at $U=5.0$ V are shown, where I_0 denotes the minimum value of I. At this bias, the current density through the OLED is 2.8×10^{-3} A/cm^2. A hysteretic behavior in I is observed with an apparent increase in I/I_0 of $\approx$0.15% for the antiparallel magnetic configuration as compared with the value for the parallel one. Superimposed on the hysteresis loop is a monotonic increase of I with the modulus of H. A magnetic-field dependence of luminescence is known for crystalline organic materials[15,16] and a positive field dependence has been recently observed for amorphous films.[17,18] An explanation of these effects is based on a magnetic-field-dependent conversion rate between singlet and triplet states.[19] We note that we see the same EL intensity modulations as shown in Fig. 1(c) if we measure at constant OLED current. We therefore exclude that these modulations are directly induced by changes in the injection current. As in Ref. 17, we find a negative magnetoresistive effect in the injection current at constant voltage. The magnetic-field-dependent modulation of the device current has a similar shape as the EL intensity shown in Fig. 1(c); its magnitude, however, is about two orders of magnitude lower.

The EL efficiency modulation induced by the electrode magnetization reversal could be interpreted as an indication of spin-polarized charge-carrier injection effects. However, we find a higher EL efficiency for the antiparallel magnetization configuration, which seems to contradict the expectation of a higher singlet-to-triplet exciton population ratio for the parallel configuration.[4] This expectation takes into account that the hole spin is opposite to that of an electron, but neglects the possibility that the two electrodes might emit spins of either majority or minority type. In fact, a higher EL efficiency for the antiparallel magnetic configuration is expected if one of the electrodes acts as a source of predomi-

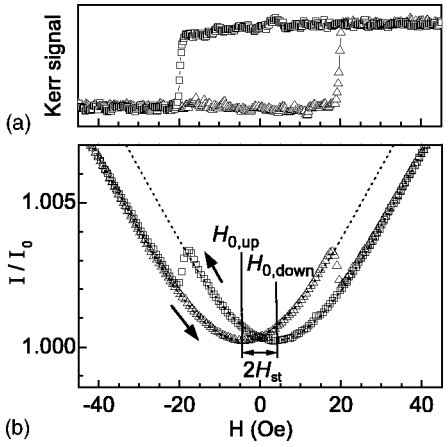

FIG. 2. (a) Longitudinal magneto-optical Kerr measurement of the OLED sample with a magnetic Ni anode and Ca cathode reveals the magnetic hysteresis of the Ni layer. (b) Corresponding OLED electroluminescence intensity I measured at $U=6.0$ V, with the up (triangles) and down sweeps (squares) falling on two different curves offset by $2H_{st}$. At magnetization reversal, I drops towards the other curve.

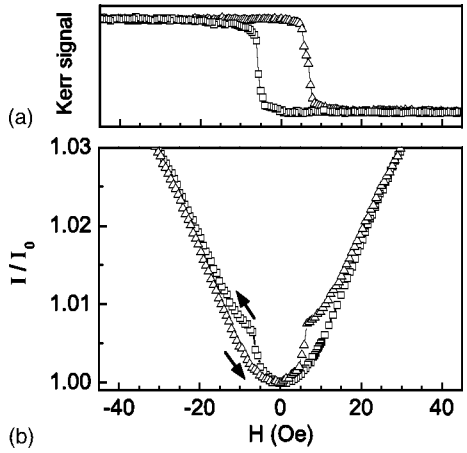

FIG. 3. (a) Longitudinal magneto-optical Kerr measurement of OLED sample with an Al anode and permalloy cathode. (b) The hysteretic OLED intensity I at $U=6.0$ V increases at magnetization reversal, followed by a slow decrease towards saturation.

nantly minority spins while the other is of the majority type. This could be the case, for example, for Ni and Fe electrodes, where the former has a predominant density of minority states near the Fermi level whereas the latter exhibits predominant majority spin one.[20,21] For the Ni and Py electrodes used here we cannot be certain of the sign of the spin polarization of the injected carriers for a number of reasons: (a) the electrodes are polycrystalline, and thus the density of states is a superposition of contributions from several crystal orientations, (b) the density of states of the FM surface can be affected by the presence of the oxide layer, and (c), the relative weighting of the states contributing to the current is determined by the injection voltage bias.

In order to understand the hysteretic EL intensity, we investigate samples with only one magnetic electrode. In such samples, no spin-dependent intensity modulation is expected because the charge carrier species injected by the nonmagnetic electrode are not spin-polarized, thus eliminating the dependence of the exciton singlet-triplet ratio on the spin polarization of the opposite carrier species. In the following, we show results from a Ni/Ca sample and an Al/Py sample.

Figure 2(a) shows hysteresis loops of the magnetization of the Ni anode of the Ni/Ca OLED, as obtained by longitudinal Kerr-effect measurements. The coercive field of the Ni layer is ~20 Oe. The EL traces are affected by the magnetic hysteresis [Fig. 2(b)]: A minimum in I occurs at different fields $H=H_{0,up}$ or $H_{0,down}$ for up or down sweeps, respectively. Starting from this minimum, I initially increases with identical shape $I(H-H_{0,i})$ for $i=$up or $i=$down [dotted lines in Fig. 2(b)]. At magnetization switching, I abruptly jumps from one curve to the other. This behavior can be understood by assuming that (i) the total magnetic field H_{tot} at the emissive region of the organic layer is composed of the applied field, H, and an additional stray field, H_{st}, originating from the magnetic electrode layer, and that (ii) the EL intensity is monotonically increasing with $|H_{tot}|$. Assumption (ii) is validated in measurements of $I(H)$ in OLEDs with nonmagnetic electrodes, where the minimum of I is reached at $H=H_{tot}=0$ (not shown). The minimum in I at $H=H_{0,up}$ and $H=H_{0,down}$ thus indicates that H_{tot} is at a minimum value at those field positions. Assuming that H_{st} is collinear with H, the jump in I at magnetization reversal is induced by a change from $H_{st}=-H_{0,up}$ to $H_{st}=-H_{0,down}$. From the data in Fig. 2(b) one obtains $H_{0,up}=6$ Oe and $H_{0,down}=-6$ Oe. This suggests that the average stray field is of magnitude 6 Oe and oriented antiparallel to H. This stray field is averaged over the volume of the emissive region of the OLED, which is located within a layer that starts at the STAD/Alq_3 interface and extends about 10 nm into the Alq_3 material. We note that the size of H_{st} is about one order of magnitude larger than expected for a demagnetizing field at a distance of 40 nm from an ideal, homogenously magnetized Ni film of thickness 50 nm and lateral extension of 2–3 mm. Possible explanations of this discrepancy are magnetic imperfections and surface roughness of the Ni film (Néel orange peel coupling[22]). This is supported by our observation that the value of H_{st} depends on the conditions of growth of the FM electrodes. Another indication that the observed H_{st} is not simply a demagnetizing field is our observation of a significant increase in H_{st} if the thickness of the organic layers is reduced by a factor of 2.

Figure 3(a) shows magnetic hysteresis loops of the sample with a Py cathode and a nonmagnetic anode. The magnetization switches at a coercive field of ~6 Oe with a more gradual transition than in the Ni/Ca sample. In Fig. 3(b), measurements of I/I_0 vs H are displayed for $U=6$ V. Similar to the Ni/Ca sample, magnetization switching affects I, but whereas in the Ni/Ca sample I decreases within a few Oe at magnetization reversal, here I increases before magnetization reversal, and then asymptotically approaches, within ~10 Oe, the values of the opposite sweep direction. From the positions of the two minima of the up and down sweeps, one obtains a stray field of ~1.5 Oe oriented against the magnetization. If the stray field were simply antiparallel to the magnetization, no increase in I would be expected at

magnetization reversal, since it would switch from an orientation parallel to H to an antiparallel one, thus reducing H_{tot}. An increase of I can only be explained by the presence of an additional stray-field contribution that increases H_{tot}, which could be induced by a stray-field component perpendicular to the applied field that builds up around magnetization reversal. A possible source for such a perpendicular stray field is the formation of domain walls around magnetization reversal leading to a correspondingly large stray field. An average perpendicular component of ~7 Oe would be needed to explain the maximum increase in I of 0.3% at $H=7$ Oe. Note that because I depends on the modulus of the magnetic field, the perpendicular stray field associated with domain walls of different sign does not cancel out. These experiments on the single magnetic layers imply that the hysteretic EL dependence can be qualitatively explained by magnetic stray fields. However, the observed differences between the Ni and the Py film show that these effects are related to the micromagnetic behavior of these films. We have performed magneto-optical Kerr microscopy studies on these films and find a different mode of magnetization reversal in Ni than in Py. Whereas in Ni the reversal is driven by domain-wall propagation, in Py it is mainly dominated by nucleation, similar to observations in ultrathin magnetic layers.[23] Correspondingly, the Py domains are much smaller, resulting in a much larger overall domain-wall length. Hence, the perpendicular stray field emanating from the domain walls is expected to be larger in Py than in Ni, in line with the EL observations. We suspect that these differences in magnetic behavior originate in the different film morphology. Scanning tunneling microscopy reveals a large roughness of the Py film with a peak-to-peak amplitude of 4 nm, and a rather flat Ni film with a roughness of less than 0.5 nm.

As will be shown in the following, also the hysteretic increase of I at the antiparallel magnetization of the Ni/Py sample [Fig. 1(c)] can be related to magnetic stray-fields. For a quantitative analysis, $I(H)$ has been measured on the Ni/Py sample for different U and fit with a Lorentz function $I=I_0[1+\Delta I/(1+H_{1/2}^2/4(H-H_{0,i})^2)]$, where ΔI is a constant, $H_{0,i}$ is the field position of minimum I, and $H_{1/2}$ is the full width at half maximum. Up and down sweeps are fitted separately using data points between −50 and −5 Oe for up sweeps (5 and 50 Oe for down sweeps). These fits describe the field-dependence of I in the region of parallel magnetization very well, as can be seen in Fig. 1(c) showing fits for $U=5.0$ V (dotted lines). Figure 4 summarizes the parameters obtained. For this sample, values of $H_{0,i}$ do not depend on U and differ by ~20 Oe for up and down sweeps [Fig. 4(a)]. As both spin-injection efficiency as well as spin transport are expected to depend on U, the constant field positions $H_{0,i}$ can not reflect spin-injection effects, but rather must be explained by the total stray field, H_{st}, being the sum of the stray fields of the Py and Ni layers. The fitted $H_{1/2}$ values [Fig. 4(b)] depend neither on U nor on the sweep direction. On the other hand, ΔI— which indicates the magnitude of the overall magnetic-field-dependent EL—monotonically decreases with U [solid line in Fig. 4(c)]. This tendency was also observed in Ref. 17.

We define two quantities, h and A, as a measure for the hysteretic behavior of $I(H)$, and compare their dependence

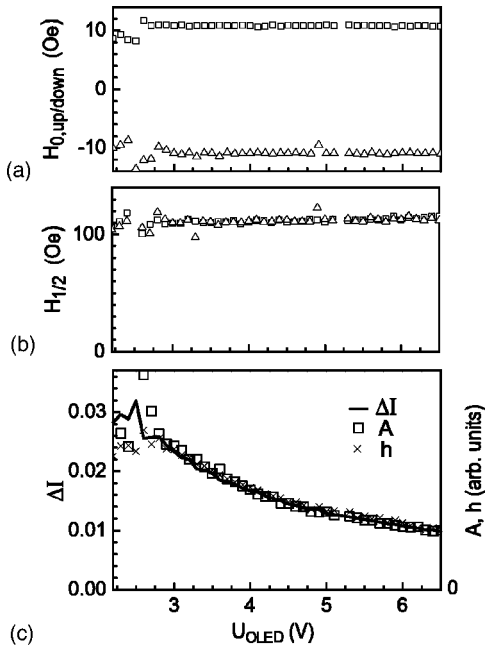

FIG. 4. Parameters of Lorentz-curve fits to measured I vs H for the Ni/permalloy OLED. Panel (a) shows the different values of H_0 for up (triangles) and down sweeps (squares), and (b) the full width at half maximum, $H_{1/2}$. These two parameters do not depend on U. (c) The total electroluminescence increase ΔI (solid line) decreases with U, with same functional form as the area A (squares) and the height h (crosses) of the intensity change at Ni magnetization reversal.

on U with the dependence of ΔI on U. Because ΔI is obtained by fitting data outside of the hysteretic range, it does not depend on the relative orientation of magnetization directions (and thus spin-injection effects). We define h as the relative change in I/I_0 at magnetization reversal of Ni [Fig. 1(c)], and A as the area obtained from the integrated difference between $I(H)/I_0$ and the extrapolated fit from the saturated magnetization region [shaded area in Fig. 1(c)]. A is a measure of the change in intensity when Py is magnetized antiparallel rather than parallel to Ni. Any spin-injection signal would be included in A. The measured values for h (crosses), A (open squares), and ΔI (line) are compared in Fig. 4(c). Both h and A are found to follow the same dependence on U as ΔI. While it is unlikely that the spin-injection efficiency is proportional to ΔI, stray-field effects automatically provide this dependence. This is because a stray-field displaces the curve $I(H)$ in field-direction by an amount that depends on the magnetic configuration, but not on U, leading to hysteretic differences in $I(H)$ that are proportional to ΔI. The observed proportionality between A and ΔI for $U>2.7$ V indicates that no significant spin injection has been achieved for these voltages. For lower U, the EL intensity becomes very faint, making it difficult to compare the dependence of A and ΔI on U.

One can quantify an upper limit for spin polarization by comparing normalized traces of $I(H)$ measured at different U. In the case of injection of charge carriers without spin correlation, $I(H)/I_0$ only depends on U through ΔI. This assumption is valid if $H_{1/2}$ and H_0 are not affected by U. Fur-

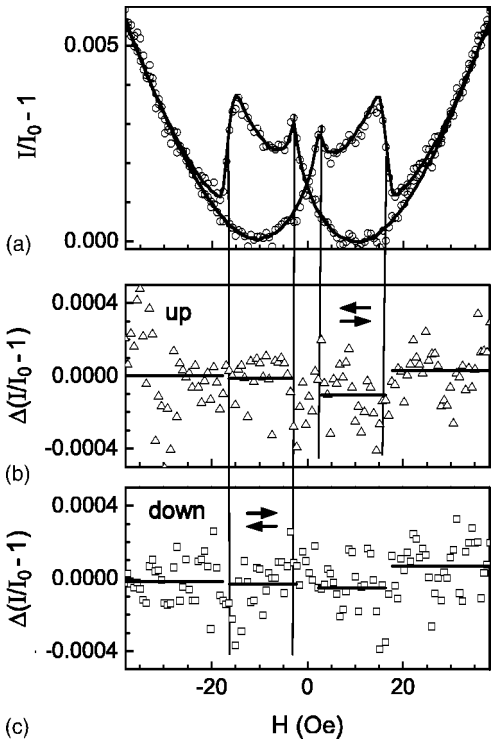

FIG. 5. (a) Relative electroluminescence intensity $(I-I_0)/I_0$ vs H for the Ni/permalloy OLED collected at 2.7 (circles) and 5.0 V (solid line). The data for 5.0 V are scaled by a factor of 2 to show that the curve matches that of the 2.7 V data. The difference between two datasets is shown for up sweeps in (b) and for down sweeps in (c) of the magnetic field. Averaging the values over antiparallel and parallel regions (solid lines) indicates a maximum change of $<10^{-4}$ due to spin injection.

thermore, we have to assume that the stray-field components of the two magnetic layers do not individually depend on U. Because of its Lorentz shape, $I(H)/I_0-1$ is directly proportional to ΔI, and different curves can be scaled by multiplying with a constant factor a. Figure 5(a) shows two curves for $U=2.7$ and 5.0 V measured on the Ni/Py sample, where the curve at 5.0 V is multiplied by $a=2.00$. The scaling factor a is given by the ratio of ΔI at 2.7 and 5.0 V, as taken from the data in Fig. 4(c). The scaled curve at 5.0 V falls on the curve at 2.7 V. A detailed analysis of the differences in the two scaled curves gives an upper limit on the spin polarization of the charge carriers. Figures 5(b) and 5(c) show the difference between the scaled intensity data at 2.7 and 5.0 V for up and down sweeps of the magnetic field. The fluctuations in the data points are mainly due to the experimental noise in the EL intensity measurement at 2.7 V. The values in Figs. 5(b) and 5(c) are averaged separately for regions with antiparallel and parallel magnetic configuration (solid lines). The averaged values deviate by less than 1×10^{-4} in intensity between the two magnetic configurations. This number can be turned into an upper limit for spin polarization. We obtain an EL intensity proportional to $1-p_e p_h$ by assuming that singlet and (nonradiating) triplet excitons form with equal probability for antiparallel electron and hole spin configuration, whereas parallel spins form nonradiating triplet excitons. Here, p_e is the electron and p_h the hole spin polarization. If at 5.0 V the spin injection is inefficient and the hysteretic EL entirely due to stray-field effects, the match of the two curves to within 1×10^{-4} gives an upper limit for $p_e p_h$ of 5×10^{-5} at $U=2.7$ V. We note that this upper limit for spin polarization is given by the noise level of the EL intensity measurements at low U.

In conclusion, we have shown that the EL of OLEDs significantly depends on magnetic fields, including stray fields from FM layers. In the search for spin injection into organic materials, the possibility that such stray fields mimic the spin effects has to be considered. We observe intensity increases for antiparallel configuration of magnetic electrodes of up to 0.3%, which would correspond to a spin polarization of both electrons and holes of ~4%. After subtracting the stray-field effect, we find an upper limit for spin polarization of $p_e p_h > 5\times10^{-5}$ for $U \geqslant 2.7$ V in the investigated samples. Further experiments will have to explore EL at lower temperatures and lower bias ranges where higher values of p_e and p_h are expected. In addition, the important role of the interface layers between the magnetic electrode and the organic material and the possibility of magnetically dead layers will have to be considered. In order to understand the details of the stray-field-induced intensity changes, spatially resolved intensity measurements will allow the differentiation to be made between averaged and local stray fields.

We acknowledge E. Lörtscher and W. Riess for allowing us to use their experimental setup, R. F. Mahrt for valuable discussions, A. Bischof and P. Müller for technical support.

[1] V. Dediu, M. Murgia, F. C. Matacotta, C. Taliani, and S. Barbanera, Solid State Commun. **122**, 181 (2002).

[2] R. Fieldering, M. Keim, G. Reuscher, W. Ossau, G. Schmidt, A. Waag, and L. W. Molenkamp, Nature (London) **402**, 787 (1999); Y. Ohno, D. K. Young, B. Beschoten, F. Matsukura, H. Ohno, and D. D. Awschalom, *ibid.* **402**, 790 (1999).

[3] *Optical Orientation*, edited by F. Meier and B. P. Zakharchenya (Elsevier, Amsterdam, 1984).

[4] A. H. Davis and K. Bussmann, J. Appl. Phys. **93**, 7358 (2003).

[5] E. Arisi, I. Bergenti, V. Dediu, M. A. Loi, M. Muccini, M. Murgia, G. Ruani, C. Taliani, and R. Zamboni, J. Appl. Phys. **93**, 7682 (2003).

[6] E. Shikoh, Y. Ando, and T. Miyazaki, J. Magn. Magn. Mater. **272**, 1921 (2004).

[7] Z. H. Xiong, Di Wu, Z. Valy Vardeny, and Jing Shi, Nature (London) **427**, 821 (2004).

[8] G. Schmidt, D. Ferrand, L. W. Molenkamp, A. T. Filip, and B. J. van Wees, Phys. Rev. B **62**, R4790 (2000).

[9] E. I. Rashba, Phys. Rev. B **62**, R16 267 (2000).

[10] X. Jiang, R. Wang, S. van Dijken, R. Shelby, R. Macfarlane, G. S.

Solomon, J. Harris, and S. S. P. Parkin, Phys. Rev. Lett. **90**, 256603 (2003).
[11] R. J. Soulen, Jr., J. M. Byers, M. S. Osofsky, B. Nadgorny, T. Ambrose, S. F. Cheng, P. R. Broussard, C. T. Tanaka, J. Nowak, J. S. Moodera, A. Barry, and J. M. D. Coey, Science **282**, 85 (1998).
[12] D. J. Monsma and S. S. P. Parkin, Appl. Phys. Lett. **77**, 720 (2000).
[13] S. F. Alvarado and W. Riess, Mater. Res. Soc. Symp. Proc. **665**, 121 (2001).
[14] S. F. Alvarado (unpublished).
[15] R. C. Johnson, R. E. Merrifield, P. Avakian, and R. B. Flippen, Phys. Rev. Lett. **19**, 285 (1967).
[16] N. E. Geacintov, M. Pope, and F. Vogel, Phys. Rev. Lett. **22**, 593 (1969).
[17] J. Kalinowski, M. Cocchi, D. Virgili, P. Di Marco, and V. Fattori, Chem. Phys. Lett. **380**, 710 (2003).
[18] E. Lörtscher, diploma thesis, ETH Zürich 2003 (unpublished).
[19] M. Pope and C. E. Swenberg, *Electronic Processes in Organic Crystals and Polymers*, 2nd ed. (Oxford University Press, New York, 1999).
[20] V. L. Moruzzi, J. F. Janak, and A. R. W. Williams, in *Calculated Electronic Properties of Metals* (Pergamon, Oxford, 1978).
[21] *Polarized Electrons in Surface Physics*, Advanced series in surface science, edited by R. Feder (Word Scientific, Singapore, 1985).
[22] L. Néel, Comptes Rendus Acad. Sci. **255**, 1676 (1962).
[23] J. Pommier, P. Meyer, G. Pénissard, J. Ferré, P. Bruno, and D. Renard, Phys. Rev. Lett. **65**, 2054 (1990).